

Mixed LOS/NLOS Mobile Station Positioning Algorithm using TOA, AOA, and Doppler-Shift

Rohan Ramlall

Department of Electrical Engineering and Computer Science

University of California, Irvine

Irvine, CA, 92697, USA

rramlall@uci.edu

Abstract—Location estimation in wireless communications systems experiencing mixed line-of-sight/non-line-of-sight (LOS/NLOS) or purely NLOS propagation paths is an open problem. In this paper, a novel least squares algorithm is presented to estimate the location of a mobile station (MS) experiencing mixed LOS/NLOS or purely NLOS communication with at least one base station (BS) by using the time of arrival (TOA), angle of arrival (AOA), and Doppler-shift (DS) measurements collected at the BS. The Cramér-Rao bound is derived and simulation results are provided to demonstrate the estimation accuracy of the proposed algorithm. It is shown that the proposed algorithm does not require proper identification of LOS and/or NLOS paths and can produce an estimate of the MS location with as little as two propagation paths between a BS and the MS.

Index Terms— Enhanced 911, localization, positioning, non-line-of-sight propagation

I. INTRODUCTION

With the proliferation of mobile devices and location-based services, location estimation in wireless communications systems has become a prominent research area in recent years. Being able to accurately locate the mobile station (MS) in wireless communication systems can be especially important in certain location-based services such as public safety, where the U.S. Federal Communication Commission has mandated the Enhanced 911 rules for cellular carriers

to provide dispatchers with information regarding the location of the caller [1]. However, location estimation in wireless communications systems experiencing mixed line-of-sight/non-line-of-sight (LOS/NLOS) or purely NLOS propagation paths is still an open problem, which is important since these types of environments are typically experienced by wireless communication systems [2]. Conventional positioning algorithms fail in severe NLOS environments because they require LOS propagation.

Many techniques in the literature have assumed the presence of both LOS and NLOS propagation paths between the base station (BS) and mobile station (MS), and have tried to identify and discard the NLOS paths; thus using only the LOS paths for location estimation [3]. Only recently have techniques tried to exploit the NLOS paths for location estimation. These include techniques that estimate the MS location in purely NLOS environments [4]-[9] and techniques that estimate the MS location in mixed LOS/NLOS or purely NLOS environments [10]-[11] using time of arrival (TOA), angle of arrival (AOA), angle of departure (AOD), and/or Doppler-shift (DS) measurements collected at the BS. The disadvantage of the purely NLOS environment techniques is that they assume no LOS propagation path exists between the BS and MS and do not properly account for the presence of any LOS paths that may be present. Furthermore, the drawback to [8]-[11] is that they use AOD which requires multiple antennas at the MS and knowledge of the orientation of the MS, which is not practical. It is practical though for multiple antennas to be present at the BS, which makes an algorithm that uses TOA, AOA, and DS measurements collected at the BS more viable than any algorithm that uses AOD measurements collected at the MS.

In this paper, a novel least squares (LS) algorithm is presented to estimate the location of a MS experiencing mixed LOS/NLOS or purely NLOS communication with at least one BS by

using the TOA, AOA, and DS measurements collected at the BS. The contributions of this paper are outlined as follows.

1) This paper extends and generalizes the approach given in [6] to account for mixed LOS/NLOS environments in addition to purely NLOS environments. The proposed algorithm consists of three steps: in the first step, LOS/NLOS identification is performed; in the second step, the location of the scatterers and speed of the MS are estimated using LS; in the third step, the location of the MS is estimated using nonlinear LS. The velocity of the MS can also be estimated using LS in an additional step.

2) A key novelty of the proposed algorithm is the system of linear equations used to solve for the location of the scatterers and speed of the MS in the second step. A similar LS algorithm in [4] estimates the location of a MS experiencing purely NLOS communication with at least one BS by using the TOA, AOA, and DS measurements collected at the BS. However, it was seen in [6] that the algorithm in [6] outperforms the algorithm in [4] in terms of MS location accuracy because of the novel system of linear equations.

3) A novel LOS/NLOS identification approach is presented based solely on the AOA of the signals received at the BS. It is seen that the identification method is not robust to large AOA measurement errors; however, it is shown that LOS paths can be approximated as NLOS paths (under the system model assumptions) and the degradation in MS location estimation performance is negligible. Hence, the proposed positioning algorithm does not require proper identification of LOS and/or NLOS paths; all paths can be treated as NLOS.

4) The Cramér-Rao bound (CRB) is clearly derived and used to assess the performance of the proposed algorithm. Furthermore, it is seen that the proposed algorithm can produce an estimate of the MS location with as little as two NLOS propagation paths received at the BS, which is

highly desirable in severe NLOS environments where conventional positioning algorithms fail because less than three LOS propagation paths are available [12].

The layout of the paper is as follows. Section II presents the system model and assumptions. Section III presents the proposed algorithm and Section IV derives the CRB. Section V presents simulation results that demonstrate the performance of the proposed algorithm in a microcellular environment. Section VI discusses the results from Section V and its implications for 5G. The paper is concluded in Section VII.

II. SYSTEM MODEL

First, the measurements observed from NLOS propagation paths between the BS and MS will be described, which will then be followed by the measurements observed from LOS propagation paths.

One BS observes N uplink communication signals from one MS. The MS is assumed to move at a constant velocity v for a period of time $N\Delta t$ (which is small, where Δt is the time between signal transmissions) while the N uplink signals are transmitted. Each of the N uplink signals arrives at the BS via S distinct paths due to the presence of S scatterers. It is assumed that all NS signals undergo a single-bounce reflection with one scatterer before arriving at the BS. Here, the term reflection refers to specular reflections [13]. Any signals that undergo multiple bounces are assumed to be attenuated enough that their contribution at the BS is negligible. This agrees with the channel models proposed in the literature [2]. It is also assumed that the clocks on the BS and MS are synchronized in time and frequency, using a technique such as two-way ranging [14]. The position of the BS is assumed to be fixed and known, and the positions of the scatterers are assumed to be fixed and unknown. Both the MS position and velocity are assumed to be unknown. Note that the model can readily be extended to cases with more than one BS.

The BS measures the TOA τ , AOA θ , and DS ζ of all NS signals. For notational simplicity, let us first look at the measurements obtained from one BS and one scatterer. From geometry, the distance between the scatterer and BS is given by

$$d_{sc,bs}(n\Delta t) = \frac{x_{sc} - x_{bs}}{\cos(\theta(n\Delta t))} = \frac{y_{sc} - y_{bs}}{\sin(\theta(n\Delta t))} \quad (1)$$

where $[x_{sc} \ y_{sc}]^T$ is the position of the scatterer, $[x_{bs} \ y_{bs}]^T$ is the position of the BS, and $\theta(n\Delta t)$ is the AOA measurement at time $n\Delta t$ of the signal arriving at the BS after reflecting off the scatterer where $n = 0, \dots, N-1$. Cross multiplying the terms in (1) produces

$$x_{sc} \sin(\theta(n\Delta t)) - y_{sc} \cos(\theta(n\Delta t)) = x_{bs} \sin(\theta(n\Delta t)) - y_{bs} \cos(\theta(n\Delta t)) \quad (2)$$

The TOA measurement at time $n\Delta t$ of the signal arriving at the BS after reflecting off the scatterer is given by

$$c\tau(n\Delta t) = \sqrt{(x_{sc} - x_{ms}(n\Delta t))^2 + (y_{sc} - y_{ms}(n\Delta t))^2} + \sqrt{(x_{sc} - x_{bs})^2 + (y_{sc} - y_{bs})^2} \quad (3)$$

for $n = 0, \dots, N-1$, where c is the propagation speed of the uplink signal (3×10^8 m/s) and $[x_{ms}(n\Delta t) \ y_{ms}(n\Delta t)]^T$ is the position of the MS at time $n\Delta t$.

The DS measurement at time $n\Delta t$ of the signal arriving at the BS after reflecting off the scatterer is given by

$$\zeta(n\Delta t) = f_R(n\Delta t) - f_T = \frac{f_T \ v_x (x_{sc} - x_{ms}(n\Delta t)) + v_y (y_{sc} - y_{ms}(n\Delta t))}{c \ \sqrt{(x_{sc} - x_{ms}(n\Delta t))^2 + (y_{sc} - y_{ms}(n\Delta t))^2}} \quad (4)$$

for $n = 0, \dots, N-1$, where f_R is the frequency of the received signal, f_T is the frequency of the transmitted signal, and $[v_x \ v_y]^T$ is the velocity of the MS. Since the BS and scatterer are both stationary, the DS observed at the BS is the same as the DS observed at the scatterer.

If a LOS propagation path exists between the BS and MS, then each of the N uplink signals arrives directly at the BS in addition to the S NLOS arrivals due to scatterers. However, note that

(1) through (4) still hold for LOS propagation paths with the following substitution $[x_{sc} \ y_{sc}]^T = [x_{bs} \ y_{bs}]^T$. At first glance, (1) and (2) might seem incorrect with the aforementioned substitution, but since $d_{sc,bs} = x_{sc} - x_{bs} = y_{sc} - y_{bs} = 0\text{m}$, it is mathematically valid to divide 0 by any nonzero quantity. This “trick” will prove to be useful in Section III.B because it maintains a parallelism in the equations pertaining to LOS paths and the equations pertaining to NLOS paths. A two-dimensional picture of a possible system is shown in Fig. 1 with 1 LOS path and $S = 2$.

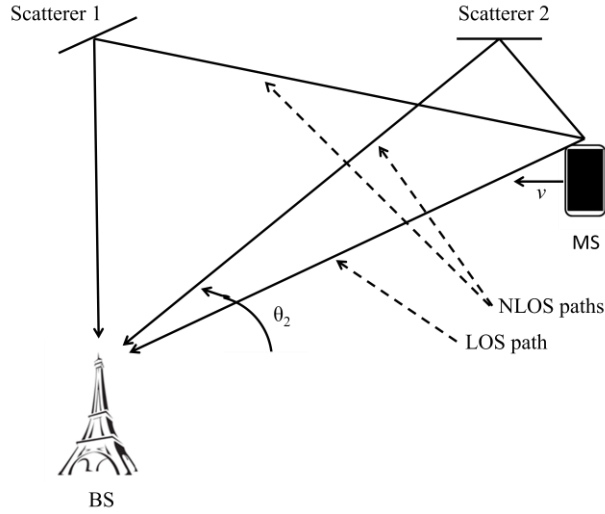


Fig. 1. Localization scenario with one BS, 1 LOS path, and 2 NLOS paths

III. PROPOSED ALGORITHM

The proposed algorithm uses the TOA, AOA, and DS measurements to estimate the MS position in three steps: LOS/NLOS identification, scatterer location and MS speed estimation, and MS position estimation. If desired, an additional step can be used to estimate the MS velocity once the MS position has been estimated.

A. LOS/NLOS Identification

The BS has no prior knowledge of which uplink signals arrived via LOS or NLOS paths, so the first step is determining which signals arrived via LOS or NLOS propagation paths. Note that the AOA from LOS paths is completely determined by the positions of the BS and MS, whereas

the AOA from NLOS paths is completely determined by the positions of the BS and scatterer. Since the BS and scatterers are fixed, the AOA is constant for the uplink signals experiencing NLOS propagation. However, due to the movement of the MS, the AOA is not constant for the uplink signals experiencing LOS propagation (unless the MS moves radially away from or towards the BS). An example is shown in Fig. 2, which shows the mean of 100 realizations of the AOA measurement arriving from a LOS path (blue) and NLOS path (red). The simulation parameters are the same as those provided later in Section V. For LOS paths, the slope of the “line” varies with each scenario, but the absolute value of the slope is greater than a threshold $a \approx 0$ (as long as the MS is not moving radially away from or towards the BS). Based on this observation, least squares is used to estimate the parameters of a line (i.e., slope and intercept) that best fits the AOA measurements arriving from each path versus time. Denote the slope of the line for path i as m_i . Then, the following test is proposed to identify whether signals arrive via LOS or NLOS paths:

$$\text{path } i \text{ is LOS: } m_i \geq a \quad (5)$$

$$\text{path } i \text{ is NLOS: } m_i < a \quad (6)$$

Note that this LOS/NLOS identification algorithm is feasible since techniques exist that can correctly associate the AOA of each path with its corresponding TOA [15]. Hence, there is no ambiguity with correctly associating which measurements correspond to which paths.

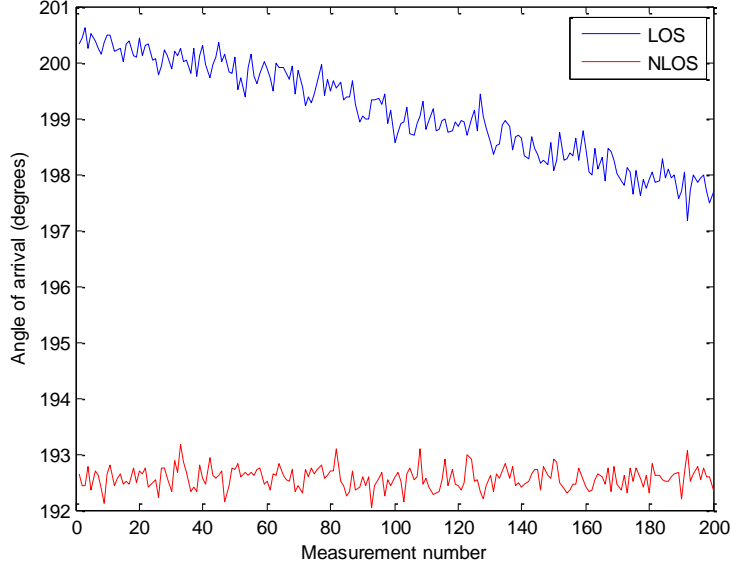


Fig. 2. Mean of 100 realizations of the AOA measurements arriving from a LOS path (blue) and NLOS path (red)

B. Scatterer Location and MS Speed Estimation

Next, the scatterer locations will be estimated for the NLOS paths. Both LOS and NLOS paths will be used to estimate the scatterer locations (see Appendix B). First, the equations produced from the LOS paths will be addressed followed by the equations produced from the NLOS paths. Utilizing (3), (4) can be written as

$$\zeta(n\Delta t) = \frac{f_T v_x (x_{sc} - (x_{ms}(0) + v_x n\Delta t)) + v_y (y_{sc} - (y_{ms}(0) + v_y n\Delta t))}{c \tau(n\Delta t) - d_{sc,bs}} \quad (7)$$

Substituting (1) into (7), and after some simplification, (7) can be written as

$$\begin{aligned} & -2 \frac{f_T}{c} v_x x_{ms}(0) - 2 \frac{f_T}{c} v_y y_{ms}(0) + \left(\zeta(n\Delta t) \sec(\theta(n\Delta t)) + 2 \frac{f_T}{c} v_x \right) x_{sc} + \left(\zeta(n\Delta t) \csc(\theta(n\Delta t)) + 2 \frac{f_T}{c} v_y \right) y_{sc} \\ & = (2c \tau(n\Delta t) + x_{bs} \sec(\theta(n\Delta t)) + y_{bs} \csc(\theta(n\Delta t))) \zeta(n\Delta t) + 2 \frac{f_T}{c} n\Delta t (v_x^2 + v_y^2) \end{aligned} \quad (8)$$

Subtracting (8) at $n = 0$ from (8) at $n = 1, \dots, N-1$ results in

$$\begin{aligned}
& (\zeta(n\Delta t)\sec(\theta(n\Delta t)) - \zeta(0)\sec(\theta(0)))x_{sc} + (\zeta(n\Delta t)\csc(\theta(n\Delta t)) - \zeta(0)\csc(\theta(0)))y_{sc} - 2\frac{f_T}{c}n\Delta t(v_x^2 + v_y^2) = \\
& (2c\tau(n\Delta t) + x_{bs}\sec(\theta(n\Delta t)) + y_{bs}\csc(\theta(n\Delta t)))\zeta(n\Delta t) - (2c\tau(0) + x_{bs}\sec(\theta(0)) + y_{bs}\csc(\theta(0)))\zeta(0)
\end{aligned} \tag{9}$$

for $n = 1, \dots, N-1$. Equations (2) and (9) are the equations that will be used later to describe the LOS paths.

For NLOS paths, (1) and (2) can be written as

$$d_{sc,bs} = \frac{x_{sc} - x_{bs}}{\cos \theta} = \frac{y_{sc} - y_{bs}}{\sin \theta} \tag{10}$$

$$x_{sc} \sin \theta - y_{sc} \cos \theta = x_{bs} \sin \theta - y_{bs} \cos \theta \tag{11}$$

respectively, where θ is the mean of the N AOA measurements of the signals arriving at the BS after reflecting off the scatterer. Following the same approach as in the derivation of (7) through (9), now using (10) instead of (1), (4) can be written as

$$\begin{aligned}
& \sec \theta (\zeta(n\Delta t) - \zeta(0))x_{sc} + \csc \theta (\zeta(n\Delta t) - \zeta(0))y_{sc} - 2\frac{f_T}{c}n\Delta t(v_x^2 + v_y^2) = \\
& (2c\tau(n\Delta t) + x_{bs}\sec \theta + y_{bs}\csc \theta)\zeta(n\Delta t) - (2c\tau(0) + x_{bs}\sec \theta + y_{bs}\csc \theta)\zeta(0)
\end{aligned} \tag{12}$$

for $n = 1, \dots, N-1$. Equations (11) and (12) are the equations that will be used subsequently to describe the NLOS paths.

Equations (2), (9), (11), and (12) can be combined for D distinct paths (the D paths are due to either the presence of S scatterers and one LOS path or S scatterers and no LOS path) to form a linear model as follows. Let $\mathbf{A}_{i,LOS}$ and $\mathbf{b}_{i,LOS}$ denote the equations corresponding to LOS path i , which are given by (13)-(14); and let $\mathbf{A}_{j,NLOS}$ and $\mathbf{b}_{j,NLOS}$ denote the equations corresponding to NLOS path j , which are given by (15)-(16).

$$\mathbf{A}_{i,LOS} = \begin{bmatrix} \sin(\theta_i(0)) & -\cos(\theta_i(0)) \\ \vdots & \vdots \\ \sin(\theta_i((N-1)\Delta t)) & -\cos(\theta_i((N-1)\Delta t)) \\ \zeta_i(\Delta t)\sec(\theta_i(\Delta t)) - \zeta_i(0)\sec(\theta_i(0)) & \zeta_i(\Delta t)\csc(\theta_i(\Delta t)) - \zeta_i(0)\csc(\theta_i(0)) \\ \vdots & \vdots \\ \zeta_i((N-1)\Delta t)\sec(\theta_i((N-1)\Delta t)) - \zeta_i(0)\sec(\theta_i(0)) & \zeta_i((N-1)\Delta t)\csc(\theta_i((N-1)\Delta t)) - \zeta_i(0)\csc(\theta_i(0)) \end{bmatrix} \quad (13)$$

$$\mathbf{b}_{i,LOS} = \begin{bmatrix} x_{bs} \sin(\theta_i(0)) - y_{bs} \cos(\theta_i(0)) \\ \vdots \\ x_{bs} \sin(\theta_i((N-1)\Delta t)) - y_{bs} \cos(\theta_i((N-1)\Delta t)) \\ (2c\tau_i(\Delta t) + x_{bs} \sec(\theta_i(\Delta t)) + y_{bs} \csc(\theta_i(\Delta t)))\zeta_i(\Delta t) - (2c\tau_i(0) + x_{bs} \sec(\theta_i(0)) + y_{bs} \csc(\theta_i(0)))\zeta_i(0) \\ \vdots \\ (2c\tau_i((N-1)\Delta t) + x_{bs} \sec((N-1)\Delta t) + y_{bs} \csc((N-1)\Delta t))\zeta_i((N-1)\Delta t) - (2c\tau_i(0) + x_{bs} \sec(\theta_i(0)) + y_{bs} \csc(\theta_i(0)))\zeta_i(0) \end{bmatrix} \quad (14)$$

$$\mathbf{A}_{j,NLOS} = \begin{bmatrix} \sin \theta_j & -\cos \theta_j \\ \sec \theta_j (\zeta_j(\Delta t) - \zeta_j(0)) & \csc \theta_j (\zeta_j(\Delta t) - \zeta_j(0)) \\ \vdots & \vdots \\ \sec \theta_j (\zeta_j((N-1)\Delta t) - \zeta_j(0)) & \csc \theta_j (\zeta_j((N-1)\Delta t) - \zeta_j(0)) \end{bmatrix} \quad (15)$$

$$\mathbf{b}_{j,NLOS} = \begin{bmatrix} x_{bs} \sin \theta_j - y_{bs} \cos \theta_j \\ (2c\tau_j(\Delta t) + x_{bs} \sec \theta_j + y_{bs} \csc \theta_j)\zeta_j(\Delta t) - (2c\tau_j(0) + x_{bs} \sec \theta_j + y_{bs} \csc \theta_j)\zeta_j(0) \\ \vdots \\ (2c\tau_j((N-1)\Delta t) + x_{bs} \sec \theta_j + y_{bs} \csc \theta_j)\zeta_j((N-1)\Delta t) - (2c\tau_j(0) + x_{bs} \sec \theta_j + y_{bs} \csc \theta_j)\zeta_j(0) \end{bmatrix} \quad (16)$$

Also define

$$\mathbf{A}_{v,LOS} = \begin{bmatrix} \mathbf{0}_{N \times 1} \\ -2 \frac{f_T}{c} \Delta t \\ \vdots \\ -2 \frac{f_T}{c} (N-1) \Delta t \end{bmatrix} \quad (17)$$

and

$$\mathbf{A}_{v,NLOS} = \begin{bmatrix} 0 \\ -2 \frac{f_T}{c} \Delta t \\ \vdots \\ -2 \frac{f_T}{c} (N-1) \Delta t \end{bmatrix} \quad (18)$$

so that the linear model is given by

$$\mathbf{A}\mathbf{s} = \mathbf{b} \quad (19)$$

where

$$\mathbf{A} = \begin{bmatrix} \mathbf{A}_{1,LOS} & & & \mathbf{A}_{v,LOS} \\ & \mathbf{A}_{1,NLOS} & & \mathbf{A}_{v,NLOS} \\ & & \ddots & \vdots \\ & & & \mathbf{A}_{S,NLOS} & \mathbf{A}_{v,NLOS} \end{bmatrix} \quad (20)$$

and

$$\mathbf{b} = [\mathbf{b}_{1,LOS} \quad \mathbf{b}_{1,NLOS} \quad \cdots \quad \mathbf{b}_{S,NLOS}]^T \quad (21)$$

if one LOS and S NLOS paths exist, or

$$\mathbf{A} = \begin{bmatrix} \mathbf{A}_{1,NLOS} & & & \mathbf{A}_{v,NLOS} \\ & \mathbf{A}_{2,NLOS} & & \mathbf{A}_{v,NLOS} \\ & & \ddots & \vdots \\ & & & \mathbf{A}_{S,NLOS} & \mathbf{A}_{v,NLOS} \end{bmatrix} \quad (22)$$

and

$$\mathbf{b} = [\mathbf{b}_{1,NLOS} \quad \mathbf{b}_{2,NLOS} \quad \cdots \quad \mathbf{b}_{S,NLOS}]^T \quad (23)$$

if no LOS and S NLOS paths exist, and

$$\mathbf{s} = [x_{sc,1} \quad y_{sc,1} \quad x_{sc,2} \quad y_{sc,2} \quad \cdots \quad x_{sc,D} \quad y_{sc,D} \quad v_x^2 + v_y^2]^T \quad (24)$$

Note that all of the entries in \mathbf{A} besides the entries shown are 0. From (19), the least squares estimate of the positions of the scatterers and squared magnitude of the MS velocity is given by

$$\hat{\mathbf{s}} = (\mathbf{A}^T \mathbf{A})^{-1} \mathbf{A}^T \mathbf{b} \quad (25)$$

C. MS Position Estimation

Now that the positions of the scatterers have been estimated, the position of the MS can be estimated at any time $n\Delta t$ for $n = 0, \dots, N-1$ as follows. The distance between the MS and scatterer i at time $n\Delta t$ is given by

$$d_i(n\Delta t) = c\tau_i(n\Delta t) - \sqrt{(x_{bs} - \hat{x}_{sc,i})^2 + (y_{bs} - \hat{y}_{sc,i})^2} \quad (26)$$

For the NLOS paths, since the signals experience LOS propagation from the MS to the scatterers and estimates of both the scatterer positions and distance between the MS and scatterers are available, the problem is now that of a conventional TOA positioning problem (along with the LOS path between the MS and BS, if present). For this paper, the author utilized the conventional iterative technique based on Taylor Series expansion [16] around an initial MS position estimate approximately equal to the position of the BS.

Finally, if desired, the scatterer position estimates from (25) and the MS position estimates from above can be substituted into (4) to solve for the MS velocity using LS.

IV. CRAMÉR-RAO BOUND

The inverse of the Fisher information matrix provides a lower bound on the covariance of any unbiased estimator of some deterministic parameter [17]. The TOA, AOA, and DS measurements can be formulated as

$$\mathbf{y} = [c\tau_1 \quad \theta_1 \quad \varsigma_1 \quad \cdots \quad c\tau_D \quad \theta_D \quad \varsigma_D]^T + \mathbf{v}^T \quad (27)$$

where τ_i , θ_i , and ζ_i are the N truth measurements corresponding to the i th path and \mathbf{v} is additive white Gaussian noise with standard deviation σ_τ , σ_θ , and σ_ζ for the TOA, AOA, and DS measurements, respectively. Looking at (27), \mathbf{y} is a multivariate Gaussian random variable with mean $\boldsymbol{\mu} = [c\tau_1 \theta_1 \zeta_1 \cdots c\tau_D \theta_D \zeta_D]^\top$ and diagonal covariance matrix \mathbf{R} . Based on the measurement model in (27), the Fisher information matrix associated with the parameter vector (28) is given by (29).

$$\mathbf{z} = [x_{sc,1} \quad y_{sc,1} \quad \cdots \quad x_{sc,D} \quad y_{sc,D} \quad v_x \quad v_y \quad x_{ms}(0) \quad y_{ms}(0)]^\top \quad (28)$$

$$\mathbf{J}(\mathbf{z}) = 2 \frac{\partial \boldsymbol{\mu}^\top}{\partial \mathbf{z}} \mathbf{R}^{-1} \frac{\partial \boldsymbol{\mu}}{\partial \mathbf{z}} \quad (29)$$

All of the derivatives needed to calculate (29) can be found in Appendix A. The CRB is obtained by inverting (29).

V. SIMULATION RESULTS

The performance of the proposed algorithm is demonstrated through Monte Carlo simulations with 1000 realizations in a microcellular environment consisting of 1 BS and 2 scatterers, resulting in 1 LOS path and 2 NLOS paths between the MS and BS. The initial position of the MS is $[x_{ms}(0) \quad y_{ms}(0)]^\top = [5000\text{m} \quad 5000\text{m}]^\top$; and the positions of the BS and scatterers are chosen according to an independent and identically distributed (i.i.d.) Gaussian random variable with mean 5000m and standard deviation $\sigma_{BS} = 1\text{km}$ and $\sigma_{SC} = 700\text{m}$, respectively. The velocity of the MS is $[v_x \quad v_y]^\top = [5\text{m/s} \quad 9\text{m/s}]^\top$, $\Delta t = 50\text{ms}$, $f_T = 2.1\text{GHz}$, and $N = 200$.

Fig. 3 through 5 show the probability that the position error is less than 100m (blue curve) and root mean square error (RMSE) (green curve) for the three types of measurement errors. Only one of the measurements at each time step has errors, while the other two are perfect. For each figure, only the type of measurement stated in the figure caption (i.e., TOA, AOA, or DS) has i.i.d. zero mean Gaussian noise with a standard deviation denoted by the x-axis and the rest of

measurements are perfect. As expected, the positioning accuracy in terms of RMSE degrades as the standard deviation of each measurement error increases. The reason the RMSE does not go to zero as the measurement error decreases is due to poor geometry of the BS, scatterers, and MS in specific Monte Carlo realizations.

Enhanced 911 requires a position accuracy of less than 100m in 67% of positioning attempts for network-based positioning methods [1]. Looking at Fig. 3 through 5, it can be seen that $\sigma_r \approx 100\text{ps}$, $\sigma_\theta \approx 50^\circ$, $\sigma_c \approx 1\text{mHz}$ are required to achieve the accuracy mandated by the Enhanced 911 positioning requirement. It should be noted that since these standard deviations were obtained assuming two of the three measurements are error free, they provide a somewhat overly optimistic view of the algorithm's performance. For example, one really needs TOA accuracy better than 100ps in order to achieve the desired accuracy when the AOA and DS measurements have errors. The reason for looking at only one error at a time is to give a fair insight into how sensitive the algorithm is to each type of measurement.

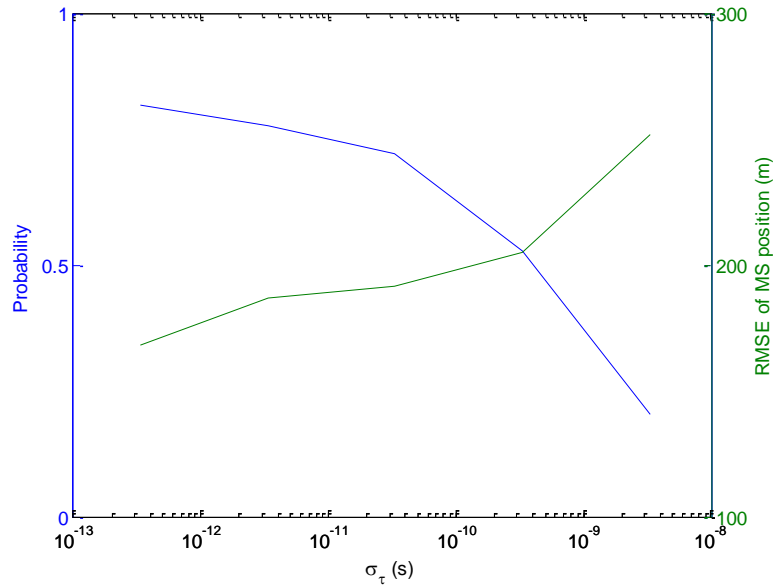


Fig. 3. E911 probability (blue) and RMSE of MS position (green) versus TOA measurement errors

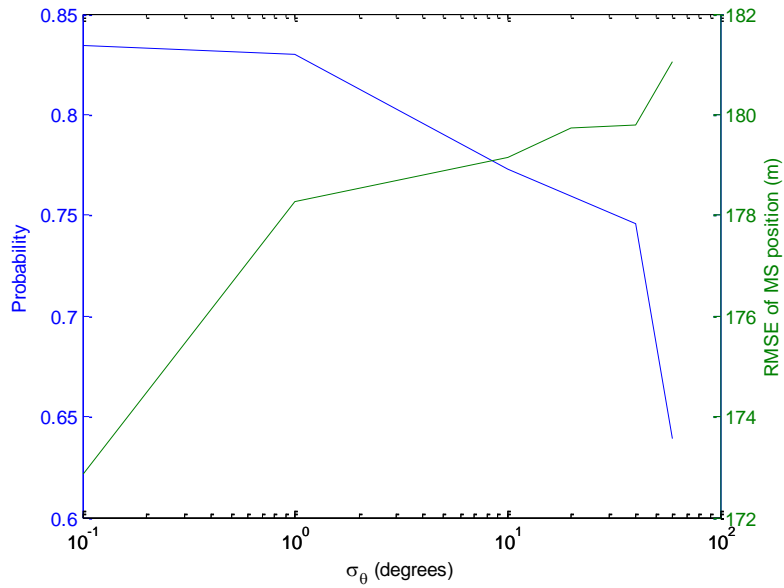


Fig. 4. E911 probability (blue) and RMSE of MS position (green) versus AOA measurement errors

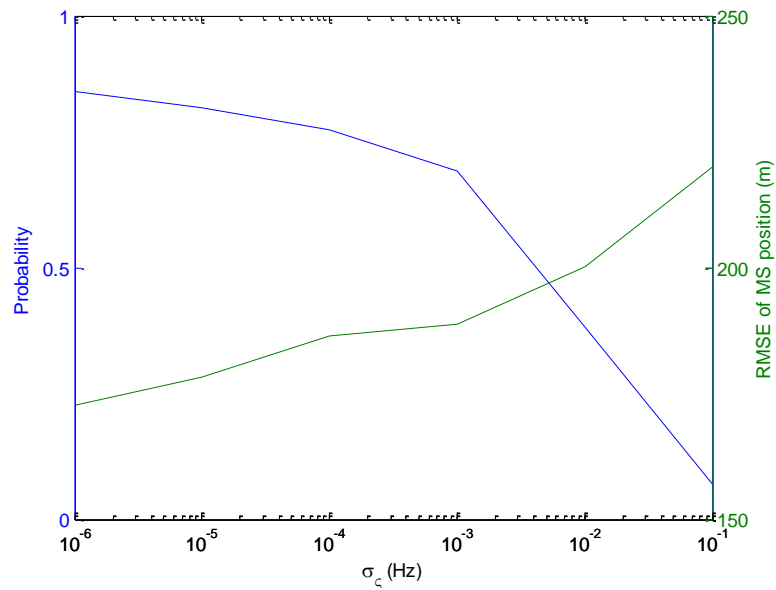


Fig. 5. E911 probability (blue) and RMSE of MS position (green) versus DS measurement errors

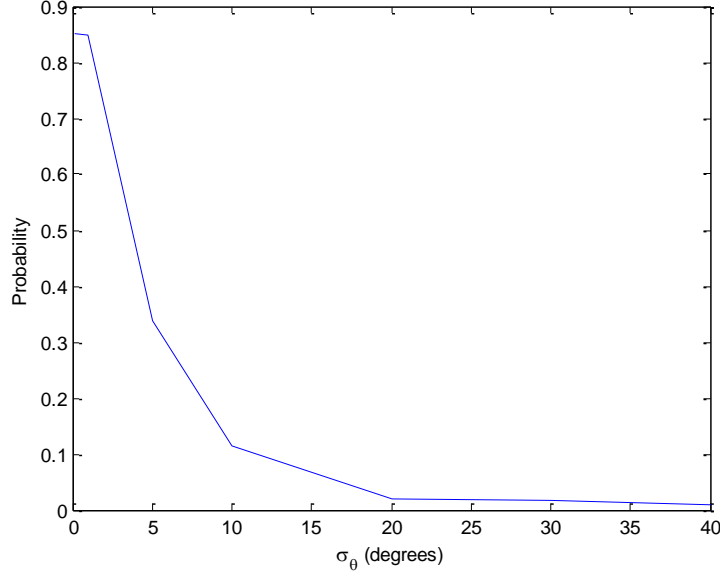


Fig. 6. LOS identification probability versus AOA measurement errors

Notice from Fig. 4 that the proposed algorithm is not sensitive to AOA errors due, in part, to the averaging of AOA measurements for NLOS paths. Fig. 6 shows the probability that the LOS path is correctly identified versus σ_θ . The proposed algorithm can satisfy the Enhanced 911 positioning requirement and not experience much degradation in RMSE performance even though its LOS identification probability degrades with increasing σ_θ , which is explained by the subsequent reasons. The first reason is that the N equations produced by (2) for a LOS path can be approximated by (11).

Proof Adding the N equations of (2) produces

$$x_{sc} \sum_{n=0}^{N-1} \sin(\theta(n\Delta t)) - y_{sc} \sum_{n=0}^{N-1} \cos(\theta(n\Delta t)) = x_{bs} \sum_{n=0}^{N-1} \sin(\theta(n\Delta t)) - y_{bs} \sum_{n=0}^{N-1} \cos(\theta(n\Delta t)) \quad (30)$$

Under the assumptions of the system model (constant MS velocity and stationary BS), (30) can be rewritten as

$$x_{sc} \sum_{k=-N/2}^{N/2} \sin(\theta + k\varepsilon) - y_{sc} \sum_{k=-N/2}^{N/2} \cos(\theta + k\varepsilon) = x_{bs} \sum_{k=-N/2}^{N/2} \sin(\theta + k\varepsilon) - y_{bs} \sum_{k=-N/2}^{N/2} \cos(\theta + k\varepsilon) \quad (31)$$

for some scalar ε . Substituting the trig identities

$$\sum_{k=-R/2}^{R/2} \sin(x + k\varepsilon) = \frac{\sin((R+1)\varepsilon/2)\sin(x + R\varepsilon/2)}{\sin(\varepsilon/2)} \quad (32)$$

$$\sum_{k=-R/2}^{R/2} \cos(x + k\varepsilon) = \frac{\sin((R+1)\varepsilon/2)\cos(x + R\varepsilon/2)}{\sin(\varepsilon/2)} \quad (33)$$

into (31), and using L'Hôpital's rule for the limit as $\varepsilon \rightarrow 0$, produces (11). \square

Since the mean value of $\varepsilon \approx 5 \times 10^{-4}$ in the 1000 Monte Carlo scenarios, the approximation of (2) with (11) is valid. The second reason is that, in many cases, the difference between each AOA measurement and the mean is small, hence using (12) instead of (9) only results in small degradation. In the 1000 scenarios, the mean and standard deviation of the maximum difference are approximately 3 and 9 degrees, respectively.

Table I provides insight into the performance of the proposed algorithm when all three measurement errors are present simultaneously. In these results, the locations of the BS and scatterers are as shown in Fig. 7, which was the best scenario out of the 1000 Monte Carlo simulations in terms of RMSE performance. Column 1 shows the measurement errors for three scenarios, Columns 2 through 5 show the square root of the MSE and CRB of the initial MS position, Column 6 shows the probability that the position error is less than 100m, and Column 7 shows the probability that the LOS path is correctly identified. Looking at Columns 2 through 5, as the measurement errors decrease, the difference between the proposed algorithm's performance (i.e., square root of the MSE) and the square root of the CRB is approximately a factor of 2. This performance gap can be accounted for because the LS estimator is not an efficient estimator for the linear system model given by (19) [18]. Also, in Section III.B, the equations (9) and (12) are obtained by subtracting measurements which increases the variance of

the measurement error. Looking at Columns 6 and 7, the proposed algorithm can still satisfy the Enhanced 911 positioning requirement even with a low LOS identification probability, as explained earlier.

TABLE I. MSE, CRB, AND E911 AND LOS ID PROBABILITIES (1 LOS AND 2 NLOS PATHS)

Scenario	\sqrt{MSE} $x_{MS(0)}$	\sqrt{CRB} $x_{MS(0)}$	\sqrt{MSE} $y_{MS(0)}$	\sqrt{CRB} $y_{MS(0)}$	E911 prob.	LOS ID prob.
$\sigma_\tau = 333\text{ps}$, $\sigma_\zeta = 5\text{mHz}$, $\sigma_\theta = 10^\circ$	29.23m	6.73m	24.38m	5.83m	0.66	0.13
$\sigma_\tau = 33\text{ps}$, $\sigma_\zeta = 1\text{mHz}$, $\sigma_\theta = 5^\circ$	6.99m	3.35m	5.59m	2.74m	0.986	0.39
$\sigma_\tau = 3.3\text{ps}$, $\sigma_\zeta = 0.1\text{mHz}$, $\sigma_\theta = 1^\circ$	1.33m	0.67m	1.0m	0.54m	1	1

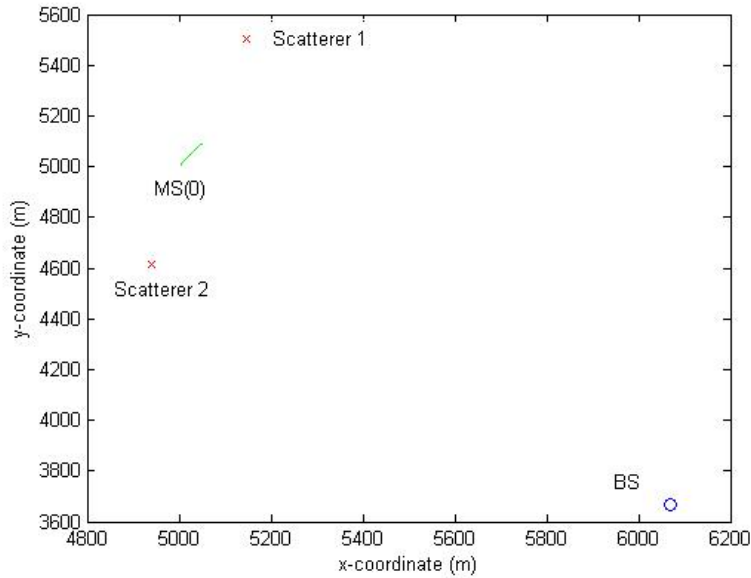


Fig. 7. Locations of BS and scatterers for the results in Table I

Lastly, Fig. 8 shows the square root of the MSE and CRB of the initial MS position for three scenarios when all three measurement errors are present simultaneously and only 2 NLOS paths are present between the MS and BS. The simulation parameters are the same as earlier with $[x_{bs} \ y_{bs}]^T = [4508.89\text{m} \ 4079.01\text{m}]^T$, $[x_{sc,1} \ y_{sc,1}]^T = [4416.74\text{m} \ 4277.98\text{m}]^T$, and $[x_{sc,2} \ y_{sc,2}]^T = [5085.94\text{m} \ 5251.15\text{m}]^T$. In scenario 1, $\sigma_\tau = 50\text{ps}$, $\sigma_\zeta = 5\text{mHz}$, and $\sigma_\theta = 20^\circ$; in scenario 2, $\sigma_\tau = 10\text{ps}$, $\sigma_\zeta = 1\text{mHz}$, and $\sigma_\theta = 10^\circ$; and in scenario 3, $\sigma_\tau = 1\text{ps}$, $\sigma_\zeta = 0.1\text{mHz}$, and $\sigma_\theta = 1^\circ$. Comparing Fig. 8 to the results in Table I show that more accurate measurements are required to obtain an accurate MS position estimate when only 2 paths are available compared to the case of when 3 paths are available. Furthermore, looking at Fig. 8, the difference between the proposed algorithm's performance and the square root of the CRB is approximately a factor of 4, which is slightly worse than before. All of this is due to less measurements being available in the 2 path case compared to the 3 path case.

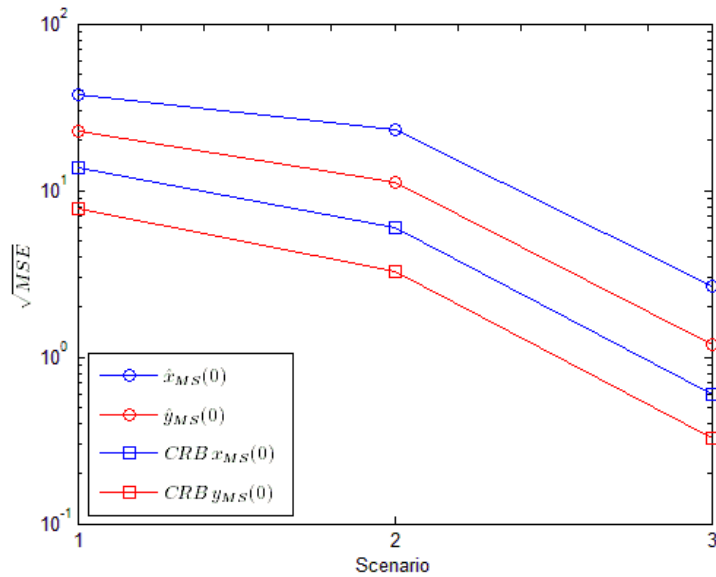


Fig. 8. MSE and CRB (2 NLOS paths)

VI. DISCUSSION

Even though the purpose of this paper is to estimate the position of the MS using TOA, AOA, and DS measurements collected at the BS, and not how to estimate the TOA, AOA, and DS measurements, a comment must be made on the feasibility of the accurate TOA and DS measurements seen in the previous section. The CRB of the TOA estimate is inversely proportional to the product of the signal-to-noise ratio (SNR) and square of the bandwidth of the uplink signal [19]; and the CRB of the DS estimate is inversely proportional to the product of the uplink signal's SNR, square of the sampling time interval, and cube of the number of uplink signal samples [20]-[21]. Hence, with sufficiently high SNR, along with other appropriate parameters (e.g., uplink signal bandwidth, number of samples collected at the BS, etc.), accurate TOA and DS measurements are indeed feasible.

The CRB of the MS position estimate also provides some interesting insights. It can be observed (using simulations), that the CRB of the MS position estimate improves as either f_T , v_x , v_y , or N increases or σ_τ , σ_ζ , or σ_θ decreases. Increasing N is limited by whether the system model assumptions are valid (e.g., constant velocity, interacting with the same scatterers, etc.), however increasing f_T has good implications for 5G where the frequencies are expected to be greater than 3GHz [23]. An interesting case is seen when the CRB is analyzed through Monte Carlo simulations with 1000 realizations in a picocellular environment consisting of 1 BS and 1 scatterer, resulting in 0 LOS paths and 1 NLOS path between the MS and BS. The simulation parameters are the same as earlier, except for the following: the positions of the BS and scatterers are chosen according to an i.i.d. Gaussian random variable with mean 5000m and standard deviation $\sigma_{BS} = \sigma_{SC} = 100\text{m}$, $[v_x \ v_y]^T = [0.6\text{m/s} \ -0.8\text{m/s}]^T$, $f_T = 10\text{GHz}$, $\sigma_\tau = 1\text{ps}$, $\sigma_\zeta = 0.1\text{mHz}$, and $\sigma_\theta = 1^\circ$. The CRB of the MS position estimate shows that it is possible to estimate

the MS position in approximately 50% of the scenarios with the square root of the CRB of the x- and y-coordinate of the initial MS position being approximately 2m. This percentage increases to over 99% if 2 NLOS paths are present, so the likely reason is poor geometry of the MS, BS, and scatterer for the 50% of scenarios that MS position estimation is not possible. MS position estimation is not possible when the same scenarios are simulated with 1 LOS path and 0 NLOS paths between the MS and BS, which further shows the advantage in position estimation that NLOS paths can provide.

VII. CONCLUSION

In this paper, a novel least squares algorithm was presented to estimate the location of a MS experiencing mixed LOS/NLOS or purely NLOS communication with at least one BS by using the TOA, AOA, and DS measurements collected at the BS. The performance of the algorithm is close to that of the CRB and it does not require proper identification of LOS and/or NLOS paths. Although the algorithm requires accurate TOA and DS measurements, a literature search revealed that these measurements are feasible for sufficiently high SNR. Finally, it was seen that the CRB of the MS location decreases as the frequency of the transmitted uplink signal increases, which has good implications for 5G.

The proposed algorithm can produce an estimate of the MS location with as little as two propagation paths between a BS and the MS. However, the CRB showed that it is sometimes possible to estimate the MS location with only 1 NLOS propagation path, which will be the subject of future work.

APPENDIX A

This appendix presents all of the derivatives needed to calculate the Fisher information matrix (29). First, the derivatives corresponding to NLOS measurements are derived. Then, the

derivatives corresponding to LOS measurements are derived. Any term not shown is equal to zero.

The derivatives corresponding to the NLOS measurements are calculated by taking the derivative of (1), (3), and (4) with respect to (28), and are given by (34)-(49). Note that (1) is formulated in terms of the arctangent function before taking the derivative.

$$\frac{\partial c \tau_i(k\Delta t)}{\partial x_{sc,i}} = \frac{x_{sc,i} - x_{ms}(k\Delta t)}{\sqrt{(x_{sc,i} - x_{ms}(k\Delta t))^2 + (y_{sc,i} - y_{ms}(k\Delta t))^2}} + \frac{x_{sc,i} - x_{bs}}{\sqrt{(x_{sc,i} - x_{bs})^2 + (y_{sc,i} - y_{bs})^2}} \quad (34)$$

$$\frac{\partial c \tau_i(k\Delta t)}{\partial y_{sc,i}} = \frac{y_{sc,i} - y_{ms}(k\Delta t)}{\sqrt{(x_{sc,i} - x_{ms}(k\Delta t))^2 + (y_{sc,i} - y_{ms}(k\Delta t))^2}} + \frac{y_{sc,i} - y_{bs}}{\sqrt{(x_{sc,i} - x_{bs})^2 + (y_{sc,i} - y_{bs})^2}} \quad (35)$$

$$\frac{\partial c \tau_i(k\Delta t)}{\partial v_x} = \frac{-x_{sc,i}k\Delta t + x_{ms}(0)k\Delta t + (k\Delta t)^2 v_x}{\sqrt{(x_{sc,i} - x_{ms}(k\Delta t))^2 + (y_{sc,i} - y_{ms}(k\Delta t))^2}} \quad (36)$$

$$\frac{\partial c \tau_i(k\Delta t)}{\partial v_y} = \frac{-y_{sc,i}k\Delta t + y_{ms}(0)k\Delta t + (k\Delta t)^2 v_y}{\sqrt{(x_{sc,i} - x_{ms}(k\Delta t))^2 + (y_{sc,i} - y_{ms}(k\Delta t))^2}} \quad (37)$$

$$\frac{\partial c \tau_i(k\Delta t)}{\partial x_{ms}(0)} = \frac{-x_{sc,i} + x_{ms}(0) + v_x k\Delta t}{\sqrt{(x_{sc,i} - x_{ms}(k\Delta t))^2 + (y_{sc,i} - y_{ms}(k\Delta t))^2}} \quad (38)$$

$$\frac{\partial c \tau_i(k\Delta t)}{\partial y_{ms}(0)} = \frac{-y_{sc,i} + y_{ms}(0) + v_y k\Delta t}{\sqrt{(x_{sc,i} - x_{ms}(k\Delta t))^2 + (y_{sc,i} - y_{ms}(k\Delta t))^2}} \quad (39)$$

$$\frac{\partial \theta_i(k\Delta t)}{\partial x_{sc,i}} = -\frac{y_{sc,i} - y_{bs}}{(x_{sc,i} - x_{bs})^2 + (y_{sc,i} - y_{bs})^2} \quad (40)$$

$$\frac{\partial \theta_i(k\Delta t)}{\partial y_{sc,i}} = \left(\frac{1}{1 + ((y_{sc,i} - y_{bs}) / (x_{sc,i} - x_{bs}))^2} \right) \left(\frac{1}{x_{sc,i} - x_{bs}} \right) \quad (41)$$

$$h(k\Delta t) = v_x (x_{sc,i} - x_{ms}(k\Delta t)) + v_y (y_{sc,i} - y_{ms}(k\Delta t)) \quad (42)$$

$$g(k\Delta t) = \sqrt{(x_{sc,i} - x_{ms}(k\Delta t))^2 + (y_{sc,i} - y_{ms}(k\Delta t))^2} \quad (43)$$

$$\frac{\partial \zeta_i(k\Delta t)}{\partial x_{sc,i}} = \frac{f_T}{c} \left(\frac{v_x}{g(k\Delta t)} - \frac{h(k\Delta t)(x_{sc,i} - x_{ms}(0) - v_x k\Delta t)}{g^3(k\Delta t)} \right) \quad (44)$$

$$\frac{\partial \zeta_i(k\Delta t)}{\partial y_{sc,i}} = \frac{f_T}{c} \left(\frac{v_y}{g(k\Delta t)} - \frac{h(k\Delta t)(y_{sc,i} - y_{ms}(0) - v_y k\Delta t)}{g^3(k\Delta t)} \right) \quad (45)$$

$$\frac{\partial \zeta_i(k\Delta t)}{\partial v_x} = \frac{f_T}{c} \left(\frac{x_{sc,i} - x_{ms}(0) - 2v_x k\Delta t}{g(k\Delta t)} - \frac{h(k\Delta t)(-x_{sc,i} k\Delta t + x_{ms}(0)k\Delta t + (k\Delta t)^2 v_x)}{g^3(k\Delta t)} \right) \quad (46)$$

$$\frac{\partial \zeta_i(k\Delta t)}{\partial v_y} = \frac{f_T}{c} \left(\frac{y_{sc,i} - y_{ms}(0) - 2v_y k\Delta t}{g(k\Delta t)} - \frac{h(k\Delta t)(-y_{sc,i} k\Delta t + y_{ms}(0)k\Delta t + (k\Delta t)^2 v_y)}{g^3(k\Delta t)} \right) \quad (47)$$

$$\frac{\partial \zeta_i(k\Delta t)}{\partial x_{ms}(0)} = \frac{f_T}{c} \left(-\frac{v_x}{g(k\Delta t)} - \frac{h(k\Delta t)(-x_{sc,i} + x_{ms}(0) + v_x k\Delta t)}{g^3(k\Delta t)} \right) \quad (48)$$

$$\frac{\partial \zeta_i(k\Delta t)}{\partial y_{ms}(0)} = \frac{f_T}{c} \left(-\frac{v_y}{g(k\Delta t)} - \frac{h(k\Delta t)(-y_{sc,i} + y_{ms}(0) + v_y k\Delta t)}{g^3(k\Delta t)} \right) \quad (49)$$

Similarly, the derivatives corresponding to the LOS measurements are calculated by taking the derivative of (1), (3), and (4) with respect to (28), except for the following modifications which are made before the derivative is taken. In (3) and (4), $[x_{sc,i} \ y_{sc,i}]^T$ is replaced with $[x_{bs} \ y_{bs}]^T$. In (1), $[x_{sc,i} \ y_{sc,i}]^T$ is replaced with $[x_{ms}(k\Delta t) \ y_{ms}(k\Delta t)]^T$. The derivatives corresponding to the LOS measurements are given by (50)-(57). Equations (36)-(39) and (44)-(49) also apply to the derivatives corresponding to the LOS measurements.

$$\frac{\partial c \tau_i(k\Delta t)}{\partial x_{sc,i}} = \frac{x_{sc,i} - x_{ms}(k\Delta t)}{\sqrt{(x_{sc,i} - x_{ms}(k\Delta t))^2 + (y_{sc,i} - y_{ms}(k\Delta t))^2}} \quad (50)$$

$$\frac{\partial c \tau_i(k\Delta t)}{\partial y_{sc,i}} = \frac{y_{sc,i} - y_{ms}(k\Delta t)}{\sqrt{(x_{sc,i} - x_{ms}(k\Delta t))^2 + (y_{sc,i} - y_{ms}(k\Delta t))^2}} \quad (51)$$

$$\frac{\partial \theta_i(k\Delta t)}{\partial x_{sc,i}} = \frac{y_{ms}(0) + v_y k\Delta t - y_{bs}}{(x_{ms}(0) + v_x k\Delta t - x_{bs})^2 + (y_{ms}(0) + v_y k\Delta t - y_{bs})^2} \quad (52)$$

$$\frac{\partial \theta_i(k\Delta t)}{\partial y_{sc,i}} = - \left(\frac{1}{1 + \left(\frac{(y_{ms}(0) + v_y k\Delta t - y_{bs})}{(x_{ms}(0) + v_x k\Delta t - x_{bs})} \right)^2} \right) \left(\frac{1}{x_{ms}(0) + v_x k\Delta t - x_{bs}} \right) \quad (53)$$

$$\frac{\partial \theta_i(k\Delta t)}{\partial v_x} = - \frac{(y_{ms}(0) + v_y k\Delta t - y_{bs}) k\Delta t}{(x_{ms}(0) + v_x k\Delta t - x_{bs})^2 + (y_{ms}(0) + v_y k\Delta t - y_{bs})^2} \quad (54)$$

$$\frac{\partial \theta_i(k\Delta t)}{\partial v_y} = \left(\frac{1}{1 + \left(\frac{(y_{ms}(0) + v_y k\Delta t - y_{bs})}{(x_{ms}(0) + v_x k\Delta t - x_{bs})} \right)^2} \right) \left(\frac{k\Delta t}{x_{ms}(0) + v_x k\Delta t - x_{bs}} \right) \quad (55)$$

$$\frac{\partial \theta_i(k\Delta t)}{\partial x_{ms}(0)} = - \frac{y_{ms}(0) + v_y k\Delta t - y_{bs}}{(x_{ms}(0) + v_x k\Delta t - x_{bs})^2 + (y_{ms}(0) + v_y k\Delta t - y_{bs})^2} \quad (56)$$

$$\frac{\partial \theta_i(k\Delta t)}{\partial y_{ms}(0)} = \left(\frac{1}{1 + \left(\frac{(y_{ms}(0) + v_y k\Delta t - y_{bs})}{(x_{ms}(0) + v_x k\Delta t - x_{bs})} \right)^2} \right) \left(\frac{1}{x_{ms}(0) + v_x k\Delta t - x_{bs}} \right) \quad (57)$$

APPENDIX B

This appendix proves that using both LOS and NLOS paths results in better estimation accuracy of the scatterer locations than only using the NLOS paths, which pertains to (19)-(21). In terms of the estimation parameter vector given by (24), path i depends on its nuisance parameters $[x_{sc,i} \ y_{sc,i}]$ and the parameter of interest $v_x^2 + v_y^2$. The LOS paths have been identified in the first step of the algorithm, so their nuisance parameters are known to be the location of the BS. However, by Theorem 1 of [22], using the measurements from the LOS path will improve the estimation performance of an efficient estimator if $\partial \boldsymbol{\mu}_{\text{LOS}} / \partial \mathbf{z}_{\text{LOS}}$ has more rows than columns and full rank 2; where $\boldsymbol{\mu}_{\text{LOS}} = [c\boldsymbol{\tau}_{\text{LOS}} \ \boldsymbol{\theta}_{\text{LOS}} \ \zeta_{\text{LOS}}]^T$ is the $3N \times 1$ vector of truth measurements corresponding to the LOS path and $\mathbf{z}_{\text{LOS}} = [x_{sc,LOS} \ y_{sc,LOS}]^T$. $\partial \boldsymbol{\mu}_{\text{LOS}} / \partial \mathbf{z}_{\text{LOS}}$ has more rows than columns if $N \geq 1$, and it is evident upon substituting (50)-(53) and (44)-(45) into $\partial \boldsymbol{\mu}_{\text{LOS}} / \partial \mathbf{z}_{\text{LOS}}$ that $\partial \boldsymbol{\mu}_{\text{LOS}} / \partial \mathbf{z}_{\text{LOS}}$ has full rank 2.

REFERENCES

- [1] The FCC, "Wireless 911 location accuracy requirements, second report and order," *FCC 10-176*, 2010.
- [2] N. Khan, M. Simsim, P. Rapajic, "A Generalized Model for the Spatial Characteristics of the Cellular Mobile Channel," *IEEE Trans. Veh. Technol.*, vol.57, no.1, pp.22-37, Jan. 2008.
- [3] I. Guvenc and C. Chong, "A survey on TOA based wireless localization and NLOS mitigation techniques," *IEEE Commun. Survey & Tutorials*, vol. 11, no.3, pp. 107–124, 3rd Quarter 2009.
- [4] K. Papakonstantinou, D. Slock, "Hybrid TOA/AOD/Doppler-Shift localization algorithm for NLOS environments," *Proc. IEEE PIMRC*, Tokyo, Japan, Sept. 2009, pp.1948-1952.
- [5] J. Chen, F. Jiang, A. Swindlehurst, J. Lopez-Salcedo, "Localization of mobile equipment in radio environments with no line-of-sight path," *Proc. IEEE ICASSP*, Vancouver, BC, Canada, May 2013, pp.4081-4085.
- [6] R. Ramlall, J. Chen, A.L. Swindlehurst, "Non-Line-of-Sight Mobile Station Positioning Algorithm using TOA, AOA, and Doppler-Shift," *IEEE UPINLBS*, to be published.
- [7] B. Shikur, T. Weber, "Localization in NLOS environments using TOA, AOD, and Doppler-shift," *Proc. IEEE WPNC*, Dresden, Germany, March 2014, pp.1-6.
- [8] X. Wei, N. Palleit, T. Weber, "AOD/AOA/TOA-based 3D Positioning in NLOS Multipath Environments," in *Proc. IEEE PIMRC*, Toronto, Canada, Sept. 2011, pp.1294–1298.
- [9] S. Chen, C. Seow, S. Tan, "Virtual Reference Device-Based NLOS Localization in Multipath Environment," *IEEE Antennas Wireless Propag. Lett.*, vol.13, pp.1409-1412, July 2014.
- [10] C. K. Seow and S. Y. Tan, "Non-line-of-sight localization in multipath environments," *IEEE Trans. Mobile Comput.*, vol. 7, no. 5, pp.647–660, May 2008.
- [11] H. Miao, K. Yu, M. Juntti, "Positioning for NLOS Propagation: Algorithm Derivations and Cramer–Rao Bounds," *IEEE Trans. Veh. Technol.*, vol.56, no.5, pp.2568-2580, Sept. 2007.
- [12] L. Yi, S. Razul, Z. Lin; C. See, "Target Tracking in Mixed LOS/NLOS Environments Based on Individual Measurement Estimation and LOS Detection," *IEEE Trans. Wireless Commun.*, vol.13, no.1, pp.99-111, Jan. 2014.
- [13] A.J. van der Veen, M. Vanderveen, A. Paulraj, "Joint angle and delay estimation using shift-invariance techniques," *IEEE Trans. Signal Process.*, vol.46, no.2, pp.405-418, Feb. 1998.

- [14] O. Bialer, D. Raphaeli, A. Weiss, "Two-Way Range Estimation Utilizing Uplink and Downlink Channels Dependency," *IEEE Trans. Signal Process.*, vol.62, no.7, pp.1619-1633, April 2014.
- [15] D. Inserra, A. Tonello, "A Frequency-Domain LOS Angle-of-Arrival Estimation Approach in Multipath Channels," *IEEE Trans. Veh. Technol.*, vol.62, no.6, pp.2812-2818, July 2013.
- [16] E. Kaplan, C. Hegarty, "Fundamentals of Satellite Navigation" in *Understanding GPS: Principles and Applications*, 2nd ed. Norwood: Artech House, 2006, ch.2, sec.4.2, pp.54-58.
- [17] T.K. Moon, W.C. Stirling, "Estimation Theory," in *Math. Methods and Algorithms for Signal Process.*, Upper Saddle River, NJ: Prentice Hall, 2000, pp.542-563.
- [18] J. Mendel, "Properties of Least-squares Estimators" in *Lessons in Estimation Theory for Signal Process., Commun., and Control*, Upper Saddle River, NJ: Prentice Hall, 2000, pp.108-117.
- [19] Y. Qi, "Wireless Geolocation in a Non-line-of-sight Environment," Ph.D. dissertation, Dept. Elect. Eng., Princeton Univ., Princeton, NJ, 2003.
- [20] P. Cheong, "Estimation of Doppler Frequency in the Presence of Noise," Defence Research Establishment Ottawa, Ottawa, ON, Technical Note 93-15, Sept. 1993.
- [21] G. Giunta, "Fast estimators of time delay and Doppler stretch based on discrete-time methods," *IEEE Trans. Signal Process.*, vol.46, no.7, pp.1785-1797, Jul 1998.
- [22] K. Papakonstantinou, D. Slock, "Identifiability and performance concerns for location estimation," *Proc. IEEE ICASSP*, Taipei, Taiwan, April 2009, pp.2097-2100.
- [23] S. Chen, J. Zhao, "The requirements, challenges, and technologies for 5G of terrestrial mobile telecommunication," *IEEE Commun. Mag.*, vol.52, no.5, pp.36-43, May 2014.